Activation of the Erk8 Mitogen-activated Protein (MAP) Kinase by RET/PTC3, a Constitutively Active Form of the RET Proto-oncogene*

Carlo Iavarone[‡1], Mario Acunzo[‡1], Francesca Carlomagno[§], Annunziata Catania[‡], Rosa M. Melillo[§],
Stella M. Carlomagno[‡], Massimo Santoro[‡], and Mario Chiariello[§2]

From the ‡Dipartimento di Biologia e Patologia Cellulare e Molecolare, Università degli Studi di Napoli "Federico II" and the
§Istituto di Endocrinologia e Oncologia Sperimentale, Consiglio Nazionale delle Ricerche (CNR), Via Pansini 5, 80131 Napoli, Italy

Mitogen-activated protein (MAP) kinases have a central role in several biological functions, including cell adhesion and spreading, chemotaxis, cell cycle progression, differentiation, and apoptosis. Extracellular signal-regulated kinase 8 (Erk8) is a large MAP kinase whose activity is controlled by serum and the c-Src non-receptor tyrosine kinase. Here, we show that RET/PTC3, an activated form of the RET proto-oncogene, was able to activate Erk8, and we demonstrate that such MAP kinase participated in RET/PTC3-dependent stimulation of the c-*jun* promoter. By using RET/PTC3 molecules mutated in specific tyrosine autophosphorylation sites, we characterized Tyr[981], a known binding site for c-Src, as a major determinant of RET/PTC3-induced Erk8 activation, although, surprisingly, the underlying mechanism did not strictly depend on the activity of Src. In contrast, we present evidence that RET/PTC3 acts on Erk8 through Tyr[981]-mediated activation of c-Abl. Furthermore, we localized the region responsible for the modulation of Erk8 activity by the RET/PTC3 and Abl oncogenes in the Erk8 C-terminal domain. Altogether, these results support a role for Erk8 as a novel effector of RET/PTC3 and, therefore, RET biological functions.

MAP[3] kinases are a family of proline-directed serine/threonine kinases that play a central role in signal transduction in all eukaryotic cells, from yeast to humans (1). They coordinate signaling from a variety of extracellular and intracellular stimuli by acting as components of modular systems that involve other kinases and regulatory proteins. These stimuli induce specific phosphorylation on a conserved Thr-Xaa-Tyr motif present in all MAP kinases, thereby inducing their activation. Consequently, these proteins transmit the signals to a vast array of cellular regulatory proteins including protein kinases, transcription factors, cytoskeletal proteins, and other enzymes (1).

Erk8 is the last identified member of the MAP kinase family of proteins (2). Expressed in humans at high levels in the brain, kidney, and lung, its activity can be modulated by serum and c-Src (2). Although possessing a very typical MAP kinase domain, Erk8 also presents a pecu-

liarly long C-terminal domain containing two putative SH3-binding sites (2). Information concerning its upstream activators, downstream effectors, and cellular functions is still extremely limited.

RET is a typical trans-membrane receptor tyrosine-kinase, essential for the development of the sympathetic, parasympathetic, and enteric nervous system and of the kidney (3). In complex with four glycosylphosphatidylinositol-anchored coreceptors, GFR-α 1–4, the RET protein binds growth factors of the glial-derived neurotrophic factor family, mediating their intracellular signaling (4). As for other receptor tyrosine-kinases, ligand interaction triggers autophosphorylation of different RET intracellular tyrosine residues that work as docking sites for several adaptor and effector signaling molecules (5). Among such tyrosines, although Tyr[981] is a binding site for c-Src, Tyr[1062] has been shown to mediate the interactions with most of RET effectors and to be responsible for activation of the Ras/Erk, phosphatidylinositol 3-kinase/Akt, Jnk, p38, and Erk5 signaling pathways (6). Finally, Tyr[1015] is a recognized docking site for phospholipase C γ (7).

Gain-of-function mutations of *RET* have been repeatedly described in several human tumors (8). *RET* germline point mutations are in fact responsible for the three clinical subtypes of the multiple endocrine neoplasias type 2 (MEN2) syndrome, MEN2A, MEN2B, and familial medullary thyroid carcinoma (5). In addition, fusion of the intracellular kinase domain of *RET* with heterologous genes, caused by chromosomal inversions or translocations, generates the *RET/PTC* oncogenes, which represent the genetic hallmark of papillary thyroid carcinomas (PTC), accounting for more than 80–90% of all thyroid carcinomas (9). Among the at least 10 different *RET/PTC* rearrangements, *RET/PTC1* and *RET/PTC3*, generated by the fusion with the *H4* and *RFG* genes, respectively, are the most common types, accounting for more than 90% of all rearrangements (10).

MATERIALS AND METHODS

Antibodies—As primary antibodies, we used rabbit polyclonal antisera to Erk2 (C-14) (Santa Cruz Biotechnology), phospho-MAPK (p42/p44) (Cell Signaling), RET and phospho-RET (phospho-Tyr905) (11), and mouse monoclonal antibodies to enhanced green fluorescent protein, AU5, and HA epitopes (Berkeley Antibody Company), Src (Ab-1; Oncogene Science), c-Abl (Pharmingen), and phospho-tyrosine, PY (Santa Cruz Biotechnology and Upstate Biotechnology).

Expression Vectors—The expression vectors pCEFLP-SrcYF (constitutively active) and pCEFLP-SrcYF KM (dominant negative) were obtained by subcloning the corresponding cDNA obtained from pSM-SrcYF and pSM-SrcYF KM, kindly provided by H. Varmus (12). The HA-tagged form of Erk8 was generated by cloning the corresponding cDNA, kindly provided by M. Abe (2), in the pCEFL-HA vector. The HA-tagged forms of Erk8 deletion mutants (1–504; 1–486; 1–386;

1–373) were generated by cloning the corresponding cDNAs, obtained by PCR amplification, in the pCEFL-HA vector. The expression vector for the dominant negative Erk8 KR molecule was also provided by M. Abe (2). To generate the pCEFL-HA-Erk8δ expression vector, we amplified by PCR the corresponding cDNA using an "expressed sequence tag" obtained from ResGen (Clone ID 5742965). These sequence data have been submitted to the GenBank™ data base under accession number AY994058. pCDNA3-RET/PTC3 and pBABE-RET/MEN2B expression plasmid have been described previously (13, 14). The RET/PTC3^{Y981}, RET/PTC3^{Y1015}, RET/PTC3^{Y1062}, RET/PTC3 Kin^{dead}, and RET/PTC3^{V804} expression plasmid were generated by the QuikChange™ site-directed mutagenesis kit (Stratagene), using pCDNA3-PTC3 as a template. Expression vectors for the activated form of c-Abl (Abl Act) and Bcr/Abl p210 (Bcr/Abl) have been described previously (15, 16). The dominant negative c-Abl (Abl-KD) expression vector was obtained by mutating a critical lysine in the kinase domain of c-Abl, contained in the pCEFL-AU5 vector. The c-*myc* and c-*jun* promoter reporter plasmids, pMyc-Luc and pJLuc, respectively, and the pCDNAIII-β-galactosidase expression vector have been described previously (12, 17). The identity and integrity of the different clones were confirmed by dideoxy DNA sequencing. For each plasmid, additional information will be provided upon request.

Western Blot Analysis—Lysates of total cellular proteins or immunoprecipitates were analyzed by protein immunoblotting after SDS-PAGE with specific rabbit antisera or mouse monoclonal antibodies. Immunocomplexes were visualized by enhanced chemiluminescence detection (ECL or ECL Plus, Amersham Biosciences) with the use of goat antiserum to rabbit or mouse immunoglobulin G, coupled to horseradish peroxidase (Amersham Biosciences).

Reagents—The PP1 inhibitor was purchased from BIOMOL. PDGF was purchased from Serologicals Corp.

Cell Culture and Transfections—293T, Cal62, Kat4, and ARO cells were maintained in Dulbecco's modified Eagle's medium supplemented with 10% fetal bovine serum, 2 mM L-glutamine, and 100 units/ml penicillin-streptomycin (Invitrogen). NIH 3T3 fibroblasts were maintained in Dulbecco's modified Eagle's medium supplemented with 10% calf bovine serum (BioWhittaker), 2 mM L-glutamine, and 100 units/ml penicillin-streptomycin (Invitrogen). Rat Pc cells were maintained in Coon's modified Ham's F12 medium supplemented with 5% calf serum and a mixture of six hormones, including 10 milliunits/ml thyrotropin, 10 nM hydrocortisone, 10 μg/ml insulin, 5 μg/ml apo-transferrin, 10 ng/ml somatostatin, and 10 ng/ml glycyl-histidyl-lysin (Sigma). 293T and NIH 3T3 cells were transfected by the Lipofectamine reagent (Invitrogen), whereas ARO cells were transfected by the Lipofectamine 2000 reagent (Invitrogen), respectively, in accordance with the manufacturer's instructions. For transfections, 200 ng of HA-Erk8 and HA-Erk8δ and 100 ng of SrcYF, Abl Act, Bcr/Abl, and of the different Ptc3 expression vectors were always used.

Reporter Gene Assays—NIH 3T3 cells were transfected with different expression plasmids together with 100 ng of the pMyc Luc reporter plasmid. ARO cells were transfected with different expression plasmids together with 20 ng of the pJLuc reporter plasmid. After a 24-h incubation in serum-free medium, the cells were lysed using reporter lysis buffer (Promega). Luciferase activity present in cellular lysates was assayed using D-luciferin and ATP as substrates, and light emission was quantitated using the 20n/20n luminometer as specified by the manufacturer (Turner BioSystems).

*RNA Extraction, RT-PCR, and Quantitative Real-time PCR*—Total RNA was isolated using the RNeasy kit (Qiagen) and subjected to on-column DNase digestion with the RNase-free DNase set (Qiagen) according to the manufacturer's instructions. The quality of RNA was verified by electrophoresis through 1% agarose gel and visualized with ethidium bromide. We synthesized random-primed first-strand cDNA in a 50-μl reaction volume starting from 2 μg of RNA using the Gene-Amp RNA PCR core kit (Applied Biosystems). Quantitative (real-time) reverse transcription-polymerase chain reactions (qRT-PCRs) were performed by using the SYBR Green PCR master mix (Applied Biosystems) in the iCycler apparatus (Bio-Rad). Amplification reactions (25-μl final reaction volume) contained 200 nM of each primer, 3 mM MgCl₂, 300 μM deoxyribonucleoside triphosphates (dNTPs), 1× SYBR Green PCR buffer (Applied Biosystems), 0.1 units/μl AmpliTaq Gold DNA Polymerase (Applied Biosystems), 0.01 units/μl Amp Erase (Applied Biosystems), RNase-free water, and 2 μl of cDNA samples. Thermal cycling conditions were optimized standard conditions and are available upon request. To verify the absence of nonspecific products, we performed 80 cycles of melting (55 °C for 10 s). The melting curve confirmed that a single product was generated. Amplification was monitored by measuring the increase in fluorescence caused by the binding of SYBR Green to double-stranded DNA. Primers were synthesized by MWG Biotech. Nucleotide sequences of the primers used in this study were as follows: qErk8Forw, 5′-GGAGTTTGGGGACCATCC-3′, and qErk8Rev, 5′-GCGTTCAGGTCAGTGTCC-3′.

Src in Vitro Kinase Assay—Cells were lysed in a buffer containing 50 mM Tris-HCl (pH 8.0), 150 mM NaCl, 1% (v/v) Nonidet P-40, 1 mM EDTA, 50 mM NaF, 20 mM sodium pyrophosphate, 1 mM sodium vanadate, 2 mM phenylmethylsulfonyl fluoride, and 0.2 mg/ml each aprotinin and leupeptin. Lysates were centrifuged at 10,000 × g for 30 min and immunoprecipitated by incubating 1 mg of total proteins with anti-Src antibodies for 60 min at 4 °C. Immunocomplexes were recovered by incubation with protein G-Sepharose beads (Amersham Biosciences) on a rotating platform at 4 °C for 60 min. After three washes with lysis buffer, the immunoprecipitates were washed with kinase buffer (20 mM Tris-HCl (pH = 7.0), 5 mM MgCl₂) and resuspended in 30 μl of kinase buffer, 10 mCi of [γ-³²P]ATP (>10,000 Ci/mmol, Amersham Biosciences), and 10 mM cold ATP. After 30 min of incubation at room temperature, the beads were washed twice with lysis buffer, and the reaction was terminated by adding an equal volume of SDS-gel loading buffer (62.5 mM Tris-HCl (pH = 6.8), 2% SDS, 5% glycerol, 0.7 M 2-mercaptoethanol, and 0.25% bromphenol blue). When indicated, 5 mg of acid-denatured enolase were added to the reaction (Roche Applied Science). The samples were electrophoresed on SDS-10% polyacrylamide gel. After the run, gels were incubated three times for 30 min in a fixing solution (20% methanol, 10% acetic acid), dried, and processed for autoradiography with phosphor screens. Laser densitometry was used to quantitate Src kinase activity.

RESULTS

Erk8 Is Activated by a RET-dependent Signaling Pathway—We performed an *in silico* analysis of *Erk8* gene expression in mouse tissues through the public Mouse Gene Prediction Database resource (18). Among other tissues, the mouse orthologue *Erk8* gene was expressed at very high levels in the thyroid. To verify *Erk8* expression also in human thyroid-derived cell lines, we next performed qRT-PCR in three human anaplastic thyroid carcinoma cell lines, ARO, Cal62, and Kat4. qRT-PCR evidenced high expression of Erk8 in the three human cell lines tested, whereas as a control, the human-specific primers did not detect any signal in a rat papillary thyroid carcinoma cell line, Pc (Fig. 1*A*). These data therefore suggest a role for Erk8 in signaling pathways involved in the homeostasis and/or pathology of the thyroid. As RET/
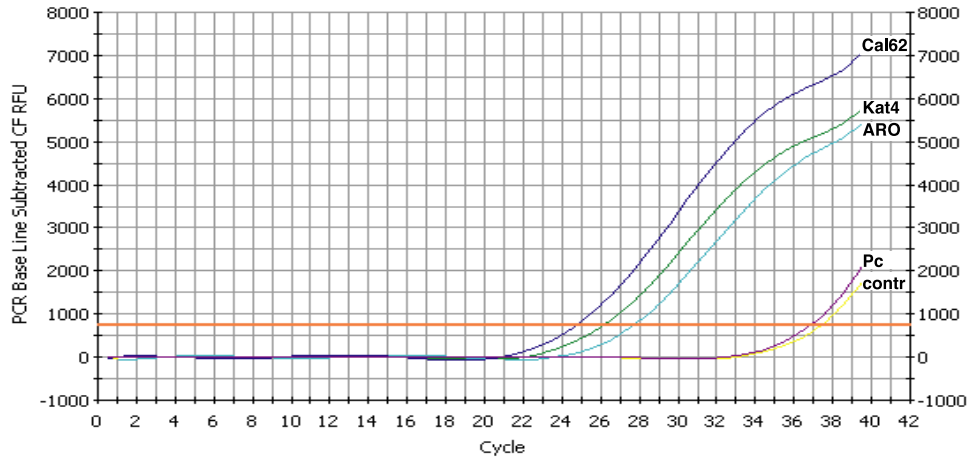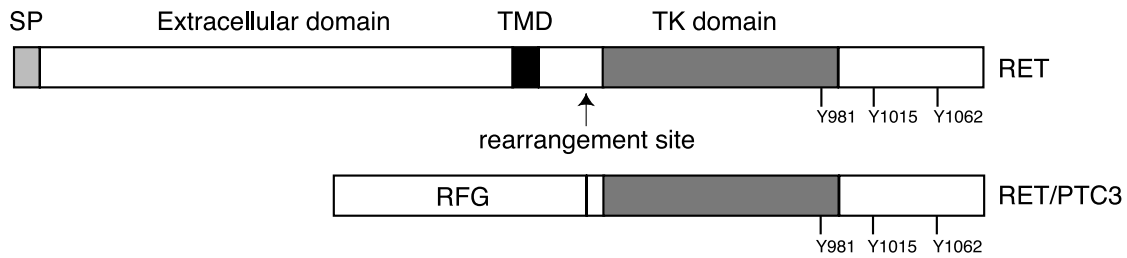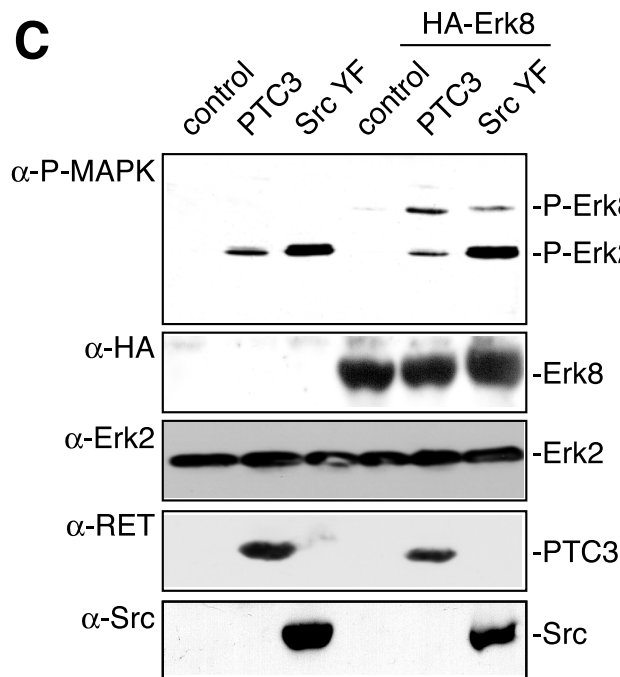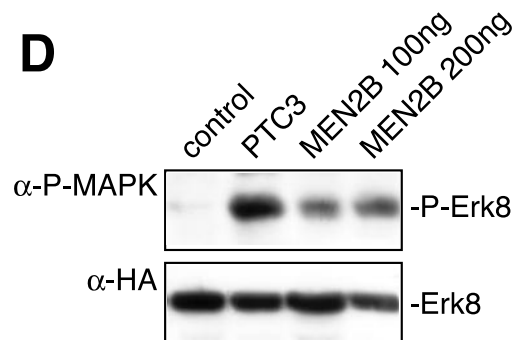
FIGURE 1. *A*, Erk8 expression in human thyroid cancer cell lines. After RNA extraction, quantitative RT-PCR was performed to evaluate Erk8 expression in human ARO, Kat4, and Cal62 cell lines. As a control (*contr*) for the specificity of the primers, rat Pc cells were also analyzed. *B*, schematic representation of the wild-type RET protein and of its activated form, the RET/PTC3 oncogene. The position of three tyrosine autophosphorylation sites and of important protein domains are also shown. *Numbers* indicating RET/PTC3 tyrosine residues correspond to their position in the wild-type RET receptor. *SP*, signal peptide; *TMD*, trans-membrane domain; *TK*, tyrosine kinase; *Y*, tyrosine; *RFG*, RET fused gene. *C*, analysis of HA-Erk8 activation in 293T cells cotransfected with the RET/PTC3 (*PTC3*) and Src YF expression vectors and analyzed by Western blot with anti-phospho MAPK (*α-P-MAPK*) antisera. Activation of endogenous Erk2 by RET/PTC3 and Src YF was used as an additional control for the activity of the two oncogenes. The expression of HA-Erk8 (*α-HA panel*), Erk2 (*α-Erk2 panel*), RET/PTC3 (*α-RET panel*), and Src YF (*α-Src panel*) was also confirmed. *P*, phospho. *D*, analysis of HA-Erk8 activation in 293T cells cotransfected with the increasing amounts of RET/MEN2B (*MEN2B*) and RET/PTC3 (*PTC3*) expression vectors and analyzed by Western blot with anti-phospho MAPK antisera. The expression of HA-Erk8 (*α-HA panel*) was confirmed. *Control*, cells transfected with β-galactosidase; *α*, anti.

PTC oncogenes are frequently involved in human papillary thyroid carcinomas (5), we decided to investigate their ability to modulate Erk8 activation. In particular, we investigated the role of RET/PTC3, a chimeric oncogene generated by the fusion of *RET* with the *RFG* gene (Fig. 1*B*) (19).

As an approach to score Erk8 activation, we used an anti-phospho-MAPK (Erk2) antibody that recognizes phosphorylation in the conserved MAP kinase TEY motif. We performed Western blot analysis of 293T cells transfected with an HA epitope-tagged form of the Erk8 kinase, as described previously by Abe *et al.* (2), and then distinguished the transfected HA-Erk8 and the endogenous Erk2 by their different molecular masses, ~60 and ~45 kDa, respectively. As shown in Fig. 1*C*, RET/PTC3 overexpression readily induced Erk8 activation at a level comparable with an activated form of c-Src (Src YF), used as a positive control (2). Of note, no signal in the ~60-kDa range was detected in the absence of HA-Erk8 transfection (Fig. 1*C*), indicating that the anti-phospho-MAPK antisera specifically recognized the Erk8 protein. As an additional control for the activity of RET/PTC3 and Src YF, both proteins activated the Erk2 MAP kinase (Fig. 1*C*), also scored by anti-phospho-MAPK Western blot.

As the RET/PTC3 oncogene is generated by the fusion of *RET* with the *RFG* gene, we next wanted to address the specific contribution of RET to the activation of the Erk8 protein. To this aim, we used a different RET-derived oncogene, RET/MEN2B, representing a specific point mutant of the intracellular RET domain (5), therefore lacking the RFG component present in the RET/PTC3 chimeric protein. As shown in Fig. 1*D*, increasing amounts of the RET/MEN2B protein also induced Erk8 activation, therefore suggesting a specific role for the RET intracellular tyrosine kinase domain in the activation of this MAP kinase. Altogether, these results indicate that activated forms of the RET proto-oncogene stimulate Erk8 activity.

A Kinase-defective Mutant for Erk8 Interferes with RET/PTC3 Signaling—The expression of the c-*jun* proto-oncogene is rapidly and transiently induced by different growth factors and cellular oncogenes (20). Among them, an oncogenic rearrangement of the RET proto-oncogene is able to strongly induce c-*jun* expression (21), therefore establishing this gene as part of the RET signaling pathway. To investigate whether the RET/PTC3 oncogene was able to stimulate the activity of the c-*jun* promoter, we took advantage of the availability of a reporter plasmid carrying the luciferase gene under the control of the c-*jun* promoter, pJLuc (17, 20).

A variety of thyroid cell lines have been used as model systems to examine RET biological functions. Among them, human anaplastic thyroid carcinoma ARO cells have the advantage to be readily transfectable and to express endogenous Erk8 (Fig. 1*A*). Cotransfection of thyroid ARO cells with the pJLuc reporter plasmid and increasing concentrations of the RET/PTC3 cDNA revealed that this oncogene could strongly induce the activity of the c-*jun* promoter (Fig. 2*A*). To evaluate whether Erk8 activation is involved in RET/PTC3 signaling to the c-*jun* promoter, we next used a dominant negative, kinase defective (data not shown) Erk8 molecule, Erk8 KR. For these experiments, we therefore cotransfected RET/PTC3 with the c-*jun* reporter plasmid and increasing amounts of the Erk8 KR expression vector. As shown in Fig. 2*B*, the dominant negative Erk8 molecule caused a strong, although incomplete, inhibition of RET/PTC3-dependent c-*jun* promoter stimulation, suggesting the existence of both Erk8-dependent and Erk8-independent pathways linking RET/PTC3 to the expression of the c-*jun* proto-oncogene.

Tyrosine 981 of RET/PTC3 Is Necessary for Erk8 Activation—Tyrosine phosphorylated residues in the kinase domain of RET, as well as of
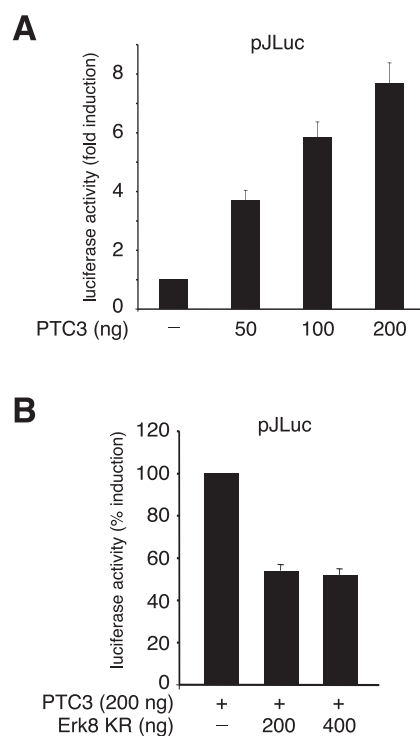

FIGURE 2. *A*, stimulation of c-*jun* promoter transcriptional activity in ARO cells transfected with the c-*jun* promoter reporter plasmid (pJLuc) and increasing concentrations of a RET/PTC3 expressing vector. *B*, c-*jun* promoter transcriptional activity in ARO cells co-transfected with pJLuc, RET/PTC3, and a Erk8 dominant negative expressing vector (*Erk8 KR*). Results represent luciferase activity in each sample, normalized for the corresponding efficiency of transfection, and they are the average ± standard errors of triplicate samples from a typical experiment.
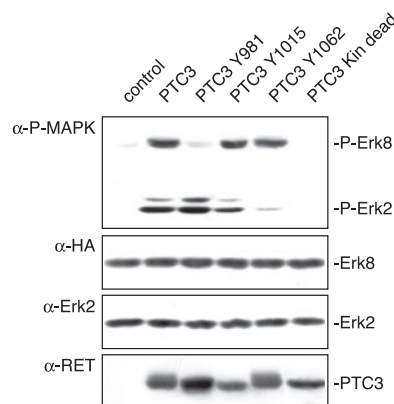

FIGURE 3. **Stimulation of Erk8 activation by RET/PTC3 (*PTC3*) and by tyrosine-mutated forms of the oncogene, in 293T cells co-transfected with an expression vector for HA-Erk8 (*α-P-MAPK panel*).** Activation of endogenous Erk2 by RET/PTC3 and its different mutated forms was used as a parallel control for the activity of the oncogenes (*α-P-MAPK panel*). The expression of HA-Erk8 (*α-HA panel*), Erk2 (*α-Erk2 panel*), and RET/PTC3 wild-type and mutants (*α-RET panel*) was also confirmed. *α*, anti; *P*, phospho; *control*, cells transfected with β-galactosidase; *Kin dead*, kinase dead.

its derivative oncogenes, usually represent docking sites for adaptor proteins and enzymes that are able to propagate the signal to the intracellular environment (5). We therefore used RET/PTC3 molecules in which different tyrosine phosphorylation sites have been inactivated by mutating them to phenylalanines to ascertain the dependence of RET/PTC3-induced Erk8 activation on the presence of these specific residues. Also, as these tyrosines have already been linked to the activation of different specific signaling pathways (5), this approach could grant us the possibility to suggest the participation of some of these effectors in the modulation of Erk8 activity. In particular, tyrosine 981 binds c-Src

FIGURE 4. *A*, the effect of PP1 on RET/PTC3^{V804} autophosphorylation (α-*P-RET panel*), in 293T cells transfected as indicated, treated for 3 h with different concentrations of the inhibitor and then analyzed by an anti-phospho RET- (α-*P-RET*) specific antisera. As a control, activation of endogenous Erk2 was also scored by Western blot with anti-phospho MAPK antisera (α-*P-MAPK panel*). Expression of RET/PTC3^{V804} and Erk2 was confirmed by Western blot performed with anti-RET and anti-Erk2 antisera, respectively (α-*RET* and α-*Erk2 panels*). *P*, phospho. *B*, same as in *A*, using RET/PTC3 to activate Erk8. *C*, Same as in *A*, analyzing RET/PTC3^{V804}-dependent Erk8 activation. *D*, the effect of PP1 on RET/PTC3^{V804}-dependent Erk8 activation (α-*P-MAPK panel*), in 293T cells transfected as indicated and pretreated with PP1 (5 μM) for increasing times. Erk8 expression was also confirmed (α-*HA panel*). *E*, the effect of PP1 on RET/PTC3^{V804}-dependent c-Src activation, in 293T cells transfected with RET/PTC3^{V804} and treated for 3 h with increasing amounts of the drug, as indicated. Laser densitometry was used to quantitate Src kinase activity, and results are expressed as a percentage relative to Src activity in cells untreated with PP1 (*c*, Me$_2$SO). The data represent the average ± standard errors of three independent experiments. *F*, analysis of Erk8 activation (*upper* α-*P-MAPK panel*) in 293T cells transfected with HA-Erk8, RET/PTC3, and increasing concentrations (250 and 500 ng) of the dominant negative Src YF KM. The expression of HA-Erk8 (α-*HA panel*) was also confirmed. *Control*, cells transfected with β-galactosidase; α, anti. *G*, inhibition of PDGF-induced c-*myc* promoter activity by Src YF KM. Stimulation of c-*myc* promoter transcriptional activity in NIH 3T3 cells transfected with the c-*myc* promoter reporter plasmid (pMyc-Luc) and a Src dominant negative expressing vectors (Src YFKM) and then stimulated for 4 h with PDGF (12.5 ng ml^{-1}) was performed. Results represent luciferase activity in each sample, normalized for the corresponding efficiency of transfection, and they are the average ± standard errors of triplicate samples from a typical experiment.
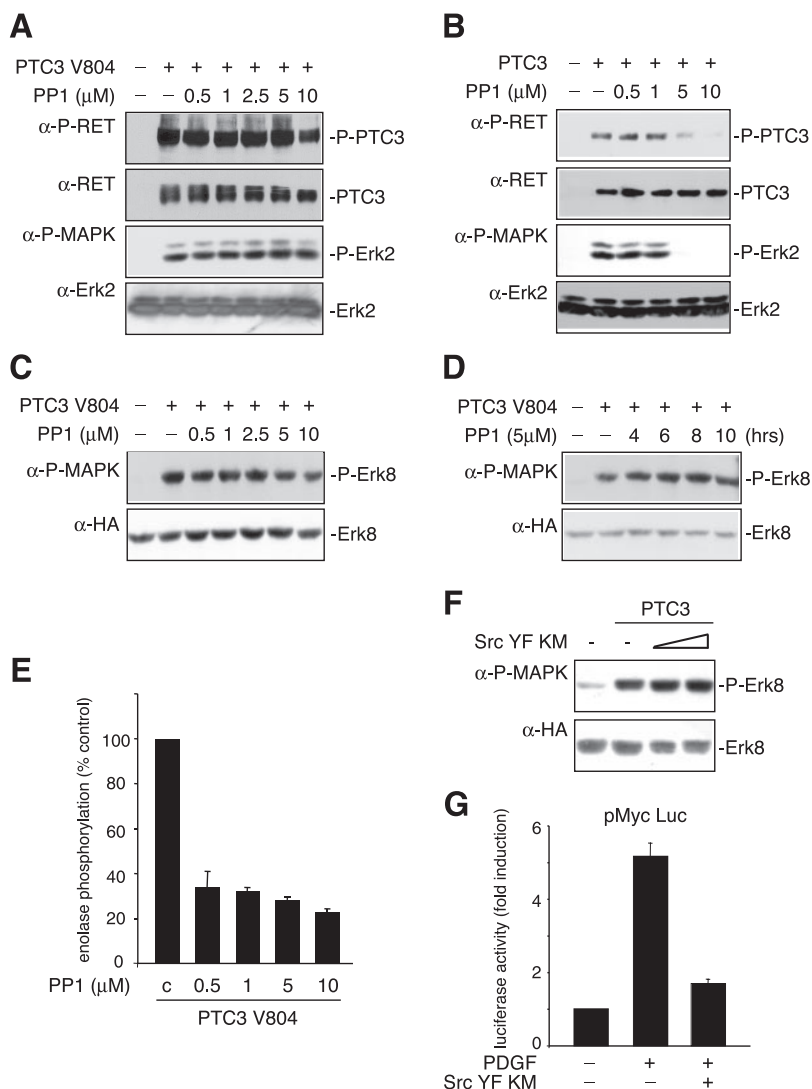
(22), tyrosine 1015 is a docking site for phospholipase C γ (7), and tyrosine 1062 is a multiple docking site that mediates most of the RET signaling pathways (6), including Erk2 activation (23). 293T cells were transiently transfected with the HA-Erk8 molecule, together with RET/PTC3, RET/PTC3^{Y981}, RET/PTC3^{Y1015}, or RET/PTC3^{Y1062}, respectively (numbers indicating RET/PTC3 tyrosine residues correspond to their position in the wild-type RET receptor). Surprisingly, based on the observation that tyrosine 1062 mediates most of the RET signaling pathways (6), the RET/PTC3^{Y1062} mutant activated Erk8 at an extent comparable with the RET/PTC3 molecule, whereas as expected (23), this mutation strongly affected Erk2 activation (Fig. 3). The tyrosine 1015 mutation, involving a known binding site for phospholipase C γ (7), also did not affect Erk8 activation by RET/PTC3 (Fig. 3). Conversely, tyrosine 981 mutation determined a dramatic reduction in RET/PTC3-dependent Erk8 activation, although such mutation proved irrelevant to Erk2 activation (Fig. 3). As a control, RET/PTC3 Kin^{dead}, a kinase-inactive form of RET/PTC3 containing a mutation in the ATP-binding catalytic lysine (Lys^{758}), was unable to activate both Erk8 and Erk2 (Fig. 3). These results therefore imply tyrosine 981 of RET/PTC3 as a major site recognized by signaling molecules mediating RET/PTC3-dependent Erk8 activation. In addition, as tyrosine 981 has been previously recognized as a key residue for the binding of c-Src to RET (22), they also

suggest a role for c-Src in mediating RET/PTC3-initiated signals impinging on Erk8 activation.

Src Activity Is Dispensable for RET/PTC3-dependent Erk8 Activation—Based on the above information and on the observation that c-Src activates Erk8 (2), we next sought to investigate whether c-Src was able to mediate RET/PTC3-dependent Erk8 activation. A classical approach to establish a role for Src kinases in cellular processes takes advantage of a pyrazolo-pyrimidine compound, PP1, which binds the ATP-binding pocket of these kinases, therefore blocking their enzymatic activity (24) and biological functions (12). Although PP1 has been described to affect RET kinase activity (25), a specific mutation in valine 804 in the RET kinase domain confers resistance (>50-fold increase of the IC$_{50}$) to the compound (11). We, therefore, introduced such mutation in the RET/PTC3 kinase domain (RET/PTC3^{V804}), rendering its activity significantly resistant to PP1, as scored by RET/PTC3^{V804} autophosphorylation and activation of Erk2 (Fig. 4*A*). As expected, kinase activity of the parental RET/PTC3 molecule was completely abolished at comparable concentrations (compare the 5–10 μM PP1 lanes) as evidenced by both RET/PTC3 autophosphorylation and activation of Erk2 (Fig. 4*B*). Surprisingly, PP1 treatment of RET/PTC3^{V804}-transfected cells only slightly affected Erk8 activity even at the highest doses tested (10 μM) (Fig. 4*C*) and after extensive times of treatment (up to 10 h of treatment,
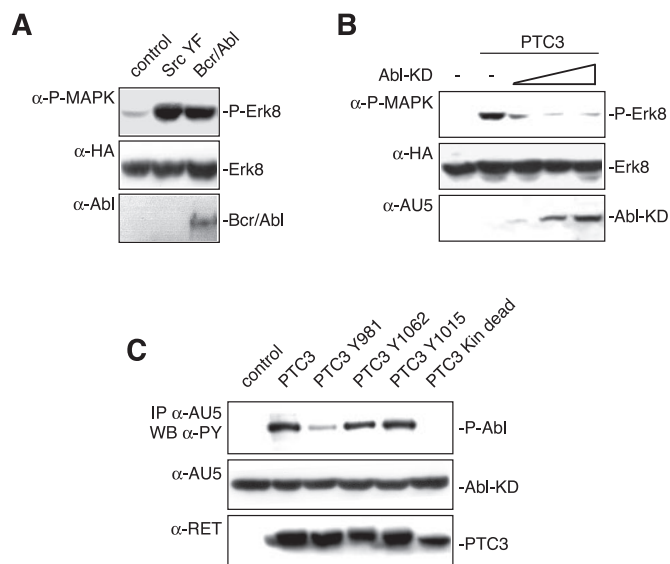
A

B

C

FIGURE 5. *A,* analysis of HA-Erk8 activation in 293T cells cotransfected with Src YF, an activated form of c-Abl, the Bcr/Abl oncogenic fusion protein. Samples were analyzed by Western blot with anti-phospho MAPK (α-P-MAPK) antisera. The expression of HA-Erk8 (α-HA panel) and Bcr/Abl (α-Abl panel) was confirmed. *Control,* cells transfected with β-galactosidase; α, anti. *B,* analysis of Erk8 activation (α-P-MAPK panel) in 293T cells transfected with HA-Erk8, RET/PTC3, and increasing concentrations (100, 250, and 500 ng) of the dominant negative Abl-KD. The expression of HA-Erk8 (α-HA panel) and of Abl-KD (α-AU5 panel) was also confirmed. *C,* stimulation of c-Abl phosphorylation by RET/PTC3 (*PTC3*) and by tyrosine-mutated forms of the oncogene. 293T cells were co-transfected with an expression vector for AU5-Abl-KD together with plasmids for RET/PTC3 and its tyrosine mutants. Samples were next immunoprecipitated (*IP*) by α-AU5 antibodies and then analyzed by α-phospho-tyrosine antibodies (α-PY). The expression of AU5-Abl-KD (α-AU5 panel) and RET/PTC3 wild-type and mutants (α-RET panel) was also confirmed. *WB,* Western blot.
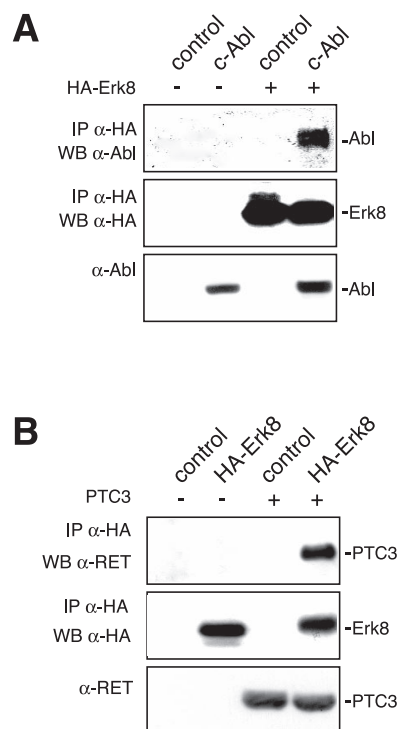
A

B

FIGURE 6. A, *In vivo* interaction of Erk8 with c-Abl. 293T cells were co-transfected with an expression vector for c-Abl (500 ng) together with plasmids for HA-Erk8 (500 ng) or control vector (β-galactosidase). Samples were next immunoprecipitated (*IP*) by anti-HA antibodies and then analyzed by anti-Abl antibodies. The expression of HA-Erk8 (*middle panel*) and c-Abl (*lower panel*) was confirmed. *WB,* Western blot. *Control,* cells transfected with β-galactosidase; α, anti. B, *in vivo* interaction of Erk8 with RET/PTC3. 293T cells were co-transfected with an expression vector for RET/PTC3 (*PTC3,* 500 ng) together with plasmids for HA-Erk8 (500 ng) or control vector (β-galactosidase). Samples were next immunoprecipitated by anti-HA antibodies and then analyzed by anti-RET antibodies. The expression of HA-Erk8 (*middle panel*) and RET/PTC3 (*lower panel*) was confirmed.

at 5 μM concentration) (Fig. 4*D*), thus excluding a role for c-Src and its related kinases (24) in the control on RET/PTC3-induced Erk8 activation. As an additional control, the PP1 inhibitor effectively disrupted Src activity in cells cotransfected with RET/PTC3^{V804} (Fig. 4*E*). As a complementary approach to ascertain the role of Src kinases in RET/PTC3 activation of Erk8, we also used a dominant negative form of c-Src, Src YF KM (12). As shown in Fig. 4*F*, overexpression of the dominant negative molecule did not affect Erk8 activation, whereas it effectively inhibited PDGF-induced activation of the c-*myc* promoter (Fig. 4*G*) (12). Altogether, these data clearly indicate that RET/PTC3 uses a Src-independent pathway to activate the Erk8 MAP kinase.

c-Abl Mediates RET/PTC3-dependent Erk8 Activation— c-Abl, the cellular homologue of the Abelson murine leukemia virus, has been implicated in different cellular processes ranging from cell growth to survival, cellular stress, DNA damage response, and cell migration (26). From the structural point of view, c-Abl contains SH3, SH2, and tyrosine kinase domains whose arrangement and sequence very much resemble that of c-Src (26). These observations prompted us to investigate whether, similarly to Src, the activated form of c-Abl could induce Erk8 activation and, in turn, whether c-Abl could mediate RET/PTC3 activation of Erk8. As shown in Fig. 5*A*, an oncogenic, activated form of c-Abl, the Bcr/Abl fusion protein, readily induced Erk8 activation at a level comparable with an activated form of c-Src (Src YF), used as a positive control (2). Thus, we next decided to investigate whether c-Abl is able to act as a link between RET/PTC3 and the stimulation of Erk8. As an approach, we used a kinase-defective, dominant negative form of c-Abl, Abl-KD. This dominant negative molecule strongly inhibited the RET/PTC3-dependent activation of Erk8 (Fig. 5*B*), thus suggesting that c-Abl is a likely mediator in the pathway connecting RET/PTC3 to the activation of the Erk8 MAP kinase.

We have previously shown that tyrosine 981 in RET/PTC3 mediates RET/PTC3-dependent Erk8 activation (Fig. 3), representing a major site recognized by signaling molecules intervening in such a process. We therefore investigated whether the tyrosine 981 residue was also able to mediate RET/PTC3 activation of c-Abl. Taking advantage of the observation that tyrosine phosphorylation of c-Abl correlates with its activation (27), we cotransfected an autophosphorylation-impaired, AU5-tagged, c-Abl molecule, together with RET/PTC3, RET/PTC3^{Y981}, RET/PTC3^{Y1015}, or RET/PTC3^{Y1062}, respectively, immunoprecipitated these samples by anti-AU5 antibodies, and analyzed them by anti-phospho-tyrosine Western blot. As show in Fig. 5*C*, RET/PTC3 clearly induced Abl phosphorylation. Importantly, RET/PTC3^{Y981} was strongly impaired in its ability to induce phosphorylation of the c-Abl protein, as compared with RET/PTC3 (Fig. 5*C*). In the same experiment, RET/PTC3^{Y1062} and RET/PTC3^{Y1015} exerted more limited or no effects, as compared with RET/PTC3 (Fig. 5*C*). Ultimately, the RET/PTC3 Kin^{dead} was unable to induce c-Abl phosphorylation, establishing a requirement for RET/PTC3 kinase activity in c-Abl activation (Fig. 5*C*). Together, these results clearly indicate that RET/PTC3, through its tyrosine 981, can utilize an Abl-dependent pathway to stimulate Erk8 activation.

Erk8 Interacts with c-Abl and RET/PTC3—To control a vast range of cellular processes, c-Abl interacts with a large variety of cellular proteins, including phosphatases, kinases, signaling adaptors, transcription factors, cytoskeletal proteins, and cell cycle regulators (26). To determine whether c-Abl can interact with Erk8 *in vivo*, 293T cells were transfected with HA-Erk8 and either wild-type c-Abl or the control vector, immunoprecipitated with an anti-HA antibody, and then analyzed by Western blot with an anti-Abl antisera. As shown in Fig. 6*A*,
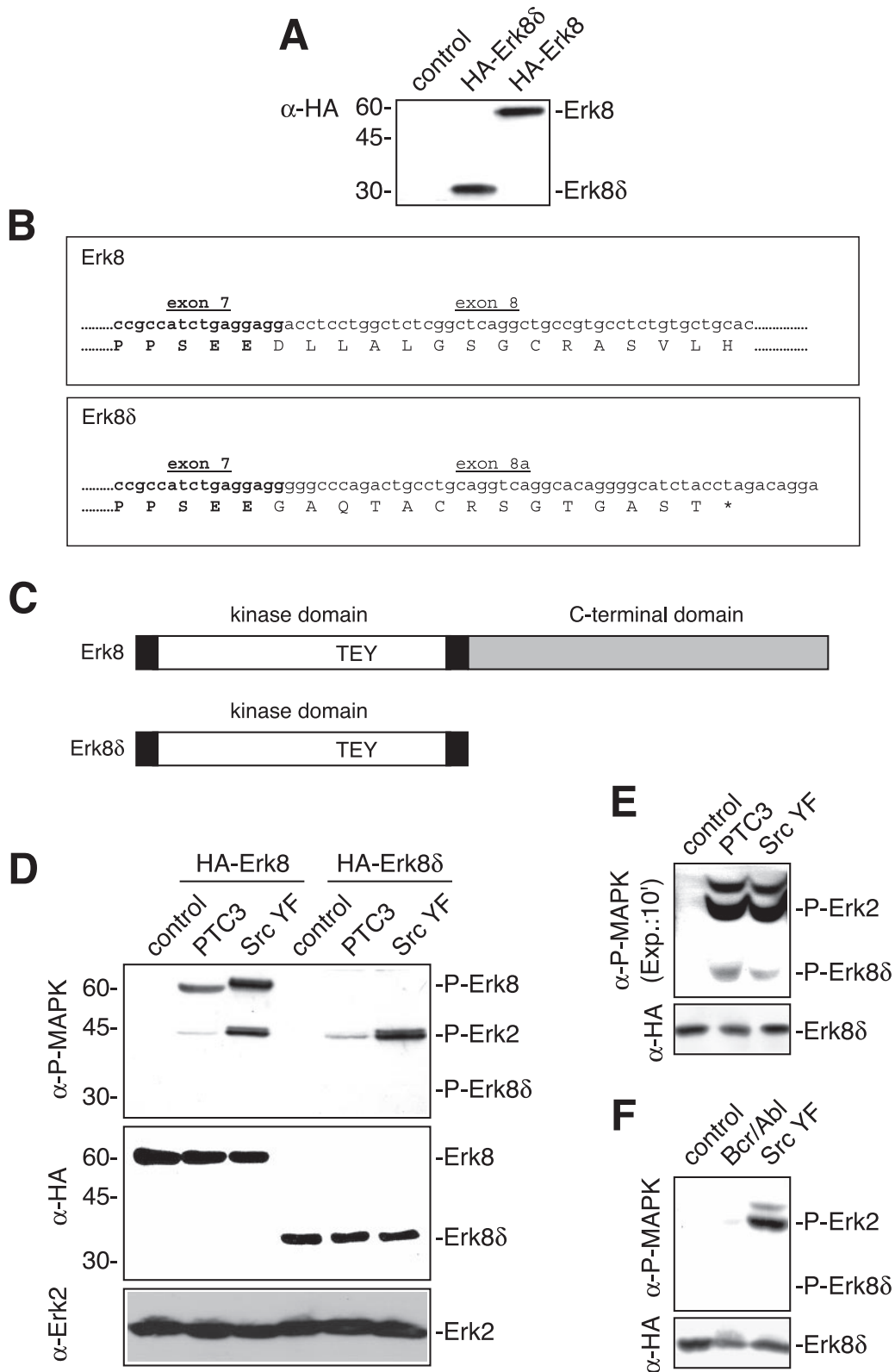
FIGURE 7. *A*, Erk8 and Erk8δ expression in transiently transfected 293T cells. *Control*, cells transfected with β-galactosidase; α, anti. *B*, comparison of Erk8 and Erk8δ nucleotide and protein sequences in the region of the alternative splicing. *C*, schematic representation of Erk8 and Erk8δ protein structures. The relative position of important residues and protein domains is indicated. *D*, analysis of Erk8 and Erk8δ activation in 293T cells cotransfected with the RET/PTC3 (*PTC3*) and Src YF expression vectors. Activation of endogenous Erk2 by RET/PTC3 and Src YF was used as an additional control for the activity of the two oncogenes. The expression of HA-Erk8, HA-Erk8δ (α-*HA panel*), and Erk2 (α-*Erk2 panel*) was also confirmed. *E*, analysis of HA-Erk8δ activation in 293T cells cotransfected with the RET/PTC3 (*PTC3*) and Src YF expression vectors and analyzed by Western blot with anti-phospho MAPK (α-*P-MAPK*) antisera. To be able to appreciate Erk8δ low levels of phosphorylation, polyvinylidene difluoride membrane was exposed 10 min after ECL reaction. The expression of HA-Erk8δ (α-*HA panel*) was confirmed. *F*, analysis of Erk8δ activation in 293T cells cotransfected with Bcr/Abl and Src YF expression vectors. The expression of HA-Erk8δ (α-*HA panel*) was confirmed.
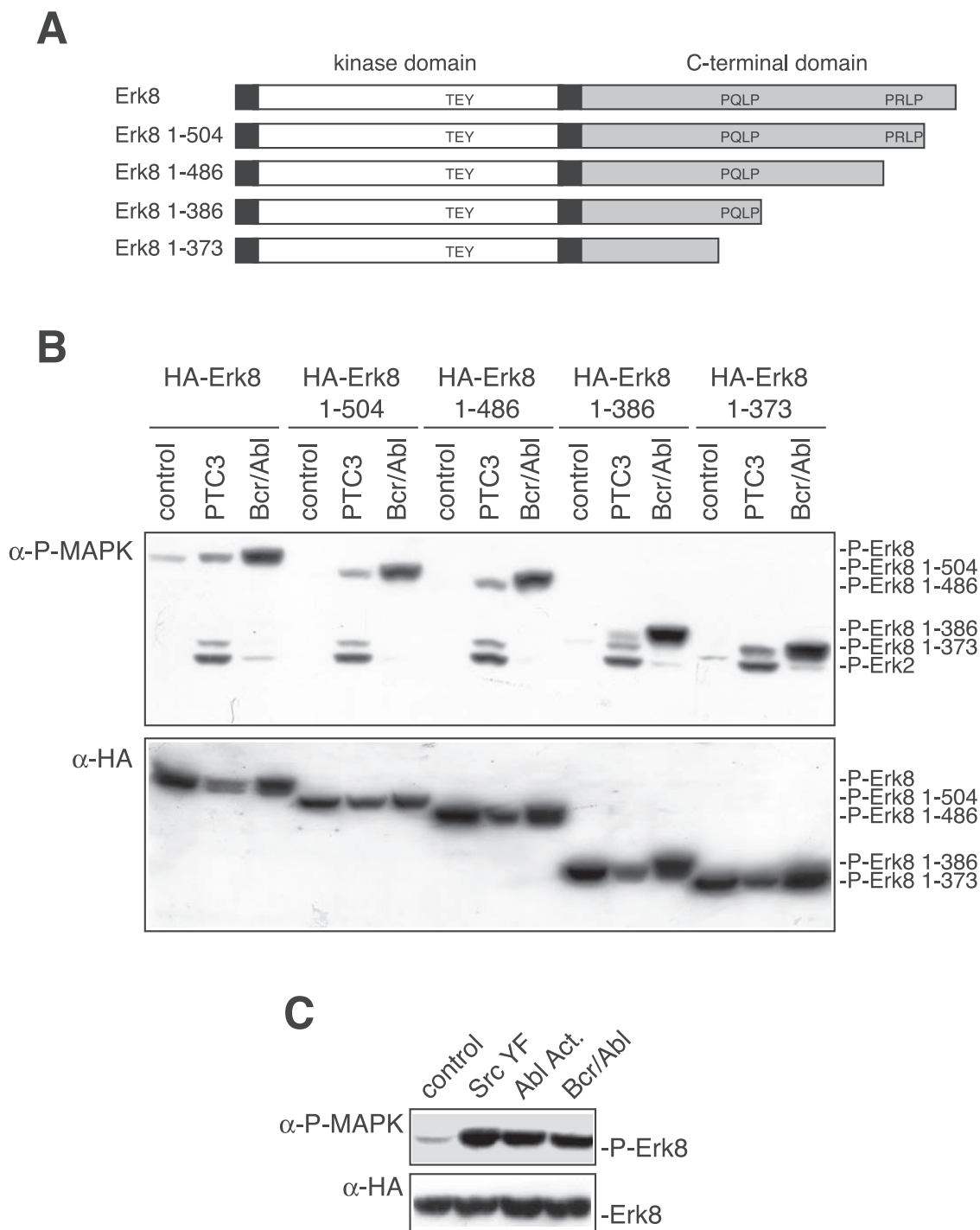
FIGURE 8. *A*, schematic representation of Erk8 protein and of its derivative C-terminal deletion mutants. The relative position of the TEY and P*XX*P motifs is also shown. *B*, analysis of the activation of Erk8 and of its derivative C-terminal deletion mutants in 293T cells cotransfected with RET/PTC3 (*PTC3*) and Bcr/Abl expression vectors. The expression of HA-Erk8 and of the different deletion mutants (*α-HA panel*) was confirmed. *C*, analysis of HA-Erk8 activation in 293T cells cotransfected with Src YF and activated forms of c-Abl, Bcr/Abl, and Abl Act. Samples were analyzed by Western blot with anti-phospho MAPK (*α-P-MAPK*) antisera. The expression of HA-Erk8 (*α-HA panel*) was confirmed. *Control*, cells transfected with β-galactosidase; *α*, anti.

c-Abl clearly co-immunoprecipitated with Erk8. In an attempt to establish a role for physical interaction in the control of Erk8 activation by RET/PTC3, we next transfected 293T cells with HA-Erk8 and either RET/PTC3 or the control vector, immunoprecipitated with an anti-HA antibody, and then analyzed by Western blot with an anti-RET antisera. Again, Erk8 evidently co-immunoprecipitated with RET/PTC3 (Fig. 6*B*), therefore suggesting the existence of a RET/PTC3-dependent mul-

tiprotein complex in which Erk8 is able to interact with both RET/PTC3 and c-Abl.

The Erk8 C-terminal Tail Modulates Activation of the MAP Kinase by RET/PTC3—Although classical MAP kinases such as Erks, Jnks, and p38s are only slightly larger than their minimum Ser/Thr kinase core, the atypical Erk5, Erk7, and Erk8 MAP kinases all contain long C-terminal domains whose functions are largely unknown. However, recent

experiments performed on Erk5 (28) and Erk7 (29) have demonstrated a role for their C-terminal tail in the regulation of kinase intracellular localization and activity. Thus, we started to investigate a role for the Erk8 C-terminal domain in RET/PTC3-dependent activation of the kinase.

The genomic organization of the *Erk8* gene has been described previously (2). By *in silico* analysis of available expressed sequence tags clones, we identified an *Erk8* cDNA whose corresponding protein, when expressed, presented a molecular mass shorter (~35 kDa) than the described Erk8 protein (~60 kDa) (Fig. 7A). We named this protein Erk8δ (accession number AY994058). Comparative analysis of the sequences for *Erk8*, *Erk8δ*, and the *Erk8* gene (NCBI Human Genome Resources) revealed that *Erk8δ* corresponded to an alternatively spliced form of *Erk8* in which an alternative exon 8 (exon 8a) contained a "stop" codon (Fig. 7B), therefore determining a 254-amino acid long protein, lacking the Erk8 C-terminal domain (Fig. 7C). Thus, we took advantage of the availability of this naturally occurring C-terminally truncated protein to evaluate the role of this domain in RET/PTC3-dependent Erk8 activation. As shown in Fig. 7D, both RET/PTC3 and Src YF were not able to induce Erk8δ activation, whereas as a control, they strongly activated Erk8. In this regard, it is important to notice that very long exposure (>10 min) of the Western blot membrane revealed that Erk8δ could still be activated by upstream stimuli (*i.e.* RET/PTC3 and Src YF) (Fig. 7E). Ultimately, the experiment depicted in Fig. 7F also demonstrated that the activated form of c-Abl, Bcr/Abl, was unable to efficiently activate Erk8δ, therefore establishing a key role for the C-terminal domain of Erk8 in the activation of this MAP kinase by various upstream stimuli.

Erk8 C-terminal SH3-binding Motifs Are Dispensable for the Activation of the MAP Kinase—Sequence analysis of Erk8 C-terminal domain revealed the presence of two potential SH3-binding motifs, P*XX*P, that are able to bind, *in vitro*, the isolated SH3 domain of c-Src fused to glutathione *S*-transferase (2). To ascertain the role of these two motifs, PQLP and PRLP, in Erk8 activation, we next prepared sequential Erk8 deletion mutants progressively lacking one or both SH3-binding sequences (Fig. 8A). Such deletion mutants were then cotransfected with RET/PTC3 and Bcr/Abl expression vectors, to score the ability of such activated oncogenes to induce their activation. As shown in Fig. 8B, RET/PTC3 and Bcr/Abl efficiently activated all tested deletion mutants, including Erk8 1–373, which lacked both SH3-binding motifs, therefore demonstrating that these domains do not affect Erk8 activation by different upstream stimuli. To further confirm this result, we also exploited an activated form of c-Abl, Abl Act, lacking the SH3 domain (30), to activate Erk8. As expected, the overexpression of this protein efficiently induced Erk8 phosphorylation (Fig. 8C), ultimately establishing that an SH3-dependent interaction is dispensable for Erk8 activation stimulated by Abl.

DISCUSSION

The complexity of the mechanisms mediating intracellular signaling by RET and its activated forms, the RET/PTC and MEN2 oncogenes, has just begun to be appreciated. Indeed, the biological functions of these proteins result from the coordinated activity of multiple kinase cascades, whose integrated signals control renal development, histogenesis of the enteric nervous system and, possibly, tumor formation (5, 8, 10). Our finding that RET/PTC3 and RET/MEN2B activate Erk8 suggests a role for this kinase in the transforming activity of RET-derived oncogenes and raises the possibility of a novel Erk8-dependent signaling pathway controlling RET biological functions.

Upon activation of different MAP kinases, a large number of tran-scription factors appears to control the expression of several growth-promoting genes, such as c-*jun* and c-*fos*, and, through these, control a vast variety of cellular functions. Specifically, the c-*jun* promoter has already been shown to represent a key site for the integration of signals coming from both cellular oncogenes (17) and extracellular ligands (20). Therefore, our observation that a dominant negative Erk8 molecule only partially inhibits the activation of the c-*jun* promoter is not surprising. Indeed, we have previously demonstrated that signaling from RET impinges on the activation of at least another MAP kinase, Jnk (23), which is able to control the activity of the c-*jun* promoter (20). We can therefore expect Erk8 to be part of the complex network of kinases, whose activation ultimately determines the specific biological response to the activation of RET and its related oncogenes in different cellular environments.

Interestingly, we have shown that Erk8 activation depends on the integrity of tyrosine 981, whereas tyrosine 1062 mutation does not affect RET/PTC3-dependent activation of the kinase. This result clearly differentiates Erk8 from other MAP kinases already involved in RET signaling whose activation, on the contrary, strictly depends on RET tyrosine 1062 (31). Although RET tyrosine 981 has been previously recognized as a docking site for c-Src (22) and this kinase modulates Erk8 activation (2), surprisingly, RET/PTC3 activation of Erk8 does not depend on c-Src. This result therefore suggests that additional molecules interact with tyrosine 981 of RET/PTC3 and are responsible for the control of Erk8 activity. Indeed, in this report, we present evidences that c-Abl controls RET/PTC3-dependent Erk8 activating phosphorylation. As a corollary to this finding, we show for the first time that c-Abl is able to mediate RET-dependent signaling pathways. Not only does RET/PTC3 induce c-Abl phosphorylation, but such a phenomenon also seems to be mediated by tyrosine 981, in line with our observation that this tyrosine mediates Erk8 activation. These findings strongly support each other, especially considering that, up to now, the only known signaling molecule downstream of this tyrosine was c-Src, whereas most of the other RET effectors depended on the integrity of tyrosine 1062.

c-Abl as well as c-Src contain well characterized SH3 domains, with a high degree of conservation in terms of sequence identity and structure (26). In c-Abl, this domain is important both for interaction with different proteins and for participation to an intramolecular regulatory mechanism (32). On the other hand, Erk8 contains two putative SH3-binding sites in its c-terminal tail (2). As the c-Src SH3 domain interacts *in vitro* with Erk8 (2), we tested the possibility that the c-Abl SH3 domain could modulate Erk8 activity. We show that deletion of the putative Erk8 SH3-binding sites does not affect the activation of the MAP kinase by both Bcr/Abl and RET/PTC3. Moreover, an activated form of c-Abl lacking the SH3 domain, Abl Act (30), efficiently induces Erk8 phosphorylation, again suggesting that an SH3-dependent interaction is dispensable for Erk8 phosphorylation. Nonetheless, it is possible that a complex between c-Abl and Erk8 may be necessary for the correct localization of the MAP kinase to particular cellular subcompartments to have full access to pools of specific substrates. Further work will be required to address these issues and to understand the role of Erk8 in RET physiological and pathological functions.

REFERENCES

1. Widmann, C., Gibson, S., Jarpe, M. B., and Johnson, G. L. (1999) *Physiol. Rev.* **79**, 143–180

2. Abe, M. K., Saelzler, M. P., Espinosa, R., III, Kahle, K. T., Hershenson, M. B., Le Beau, M. M., and Rosner, M. R. (2002) *J. Biol. Chem.* **277,** 16733–16743

3. Schuchardt, A., D'Agati, V., Larsson-Blomberg, L., Costantini, F., and Pachnis, V. (1994) *Nature* **367,** 380–383

4. Airaksinen, M. S., and Saarma, M. (2002) *Nat. Rev. Neurosci.* **3,** 383–394

5. Santoro, M., Melillo, R. M., Carlomagno, F., Vecchio, G., and Fusco, A. (2004) *Endocrinology* **145,** 5448–5451

6. Kurokawa, K., Kawai, K., Hashimoto, M., Ito, Y., and Takahashi, M. (2003) *J. Intern. Med.* **253,** 627–633

7. Borrello, M. G., Alberti, L., Arighi, E., Bongarzone, I., Battistini, C., Bardelli, A., Pasini, B., Piutti, C., Rizzetti, M. G., Mondellini, P., Radice, M. T., and Pierotti, M. A. (1996) *Mol. Cell. Biol.* **16,** 2151–2163

8. Pasini, B., Ceccherini, I., and Romeo, G. (1996) *Trends Genet* **12,** 138–144

9. Sherman, S. I. (2003) *Lancet* **361,** 501–511

10. Nikiforov, Y. E. (2002) *Endocr. Pathol.* **13,** 3–16

11. Carlomagno, F., Guida, T., Anaganti, S., Vecchio, G., Fusco, A., Ryan, A. J., Billaud, M., and Santoro, M. (2004) *Oncogene* **23,** 6056–6063

12. Chiariello, M., Marinissen, M. J., and Gutkind, J. S. (2001) *Nat. Cell Biol.* **3,** 580–586

13. Carlomagno, F., De Vita, G., Berlingieri, M. T., de Franciscis, V., Melillo, R. M., Colantuoni, V., Kraus, M. H., Di Fiore, P. P., Fusco, A., and Santoro, M. (1996) *EMBO J.* **15,** 2717–2725

14. Melillo, R. M., Santoro, M., Ong, S. H., Billaud, M., Fusco, A., Hadari, Y. R., Schlessinger, J., and Lax, I. (2001) *Mol. Cell. Biol.* **21,** 4177–4187

15. Lobo, V., Luquero, C. I. A., Alvarez-Vallina, L., Tipping, A. J., Viniegra, J. G., Losa, J. H., Cobo, C. P., Moya, E. M. G., Cruz, J. G., Melo, J. V., Cajal, S. R. Y., and Sanchez-Prieto, R. (2005) *Biochem. J.* **387,** 231–238

16. Sanchez-Prieto, R., Sanchez-Arevalo, V. J., Servitja, J. M., and Gutkind, J. S. (2002) *Oncogene* **21,** 974–979

17. Chiariello, M., Marinissen, M. J., and Gutkind, J. S. (2000) *Mol. Cell. Biol.* **20,** 1747–1758

18. Zhang, W., Morris, Q. D., Chang, R., Shai, O., Bakowski, M. A., Mitsakakis, N., Mohammad, N., Robinson, M. D., Zirngibl, R., Somogyi, E., Laurin, N., Eftekharpour, E., Sat, E., Grigull, J., Pan, Q., Peng, W. T., Krogan, N., Greenblatt, J., Fehlings, M., van der Kooy, D., Aubin, J., Bruneau, B. G., Rossant, J., Blencowe, B. J., Frey, B. J., and Hughes, T. R. (2004) *J. Biol.* (*Bronx N. Y.*) **3,** 21

19. Santoro, M., Dathan, N. A., Berlingieri, M. T., Bongarzone, I., Paulin, C., Grieco, M., Pierotti, M. A., Vecchio, G., and Fusco, A. (1994) *Oncogene* **9,** 509–516

20. Marinissen, M. J., Chiariello, M., Pallante, M., and Gutkind, J. S. (1999) *Mol. Cell. Biol.* **19,** 4289–4301

21. Ishizaka, Y., Takahashi, M., Ushijima, T., Sugimura, T., and Nagao, M. (1991) *Biochem. Biophys. Res. Commun.* **179,** 1331–1336

22. Encinas, M., Crowder, R. J., Milbrandt, J., and Johnson, E. M., Jr. (2004) *J. Biol. Chem.* **279,** 18262–18269

23. Chiariello, M., Visconti, R., Carlomagno, F., Melillo, R. M., Bucci, C., de Franciscis, V., Fox, G. M., Jing, S., Coso, O. A., Gutkind, J. S., Fusco, A., and Santoro, M. (1998) *Oncogene* **16,** 2435–2445

24. Hanke, J. H., Gardner, J. P., Dow, R. L., Changelian, P. S., Brissette, W. H., Weringer, E. J., Pollok, B. A., and Connelly, P. A. (1996) *J. Biol. Chem.* **271,** 695–701

25. Carlomagno, F., Vitagliano, D., Guida, T., Napolitano, M., Vecchio, G., Fusco, A., Gazit, A., Levitzki, A., and Santoro, M. (2002) *Cancer Res.* **62,** 1077–1082

26. Hantschel, O., and Superti-Furga, G. (2004) *Nat. Rev. Mol. Cell Biol.* **5,** 33–44

27. Plattner, R., Kadlec, L., DeMali, K. A., Kazlauskas, A., and Pendergast, A. M. (1999) *Genes Dev.* **13,** 2400–2411

28. Buschbeck, M., and Ullrich, A. (2005) *J. Biol. Chem.* **280,** 2659–2667

29. Abe, M. K., Kahle, K. T., Saelzler, M. P., Orth, K., Dixon, J. E., and Rosner, M. R. (2001) *J. Biol. Chem.* **276,** 21272–21279

30. Mayer, B. J., and Baltimore, D. (1994) *Mol. Cell. Biol.* **14,** 2883–2894

31. Hayashi, H., Ichihara, M., Iwashita, T., Murakami, H., Shimono, Y., Kawai, K., Kurokawa, K., Murakumo, Y., Imai, T., Funahashi, H., Nakao, A., and Takahashi, M. (2000) *Oncogene* **19,** 4469–4475

32. Wang, J. Y. J. (2004) *Nat. Cell Biol.* **6,** 3–7